JB
Journals.ASM.org

Identification of Three Noncontiguous Regions on *Bacillus anthracis* Plasmid pXO1 That Are Important for Its Maintenance

Andrei P. Pomerantsev, Zanetta Chang, Catherine Rappole, Stephen H. Leppla

National Institute of Allergy and Infectious Diseases, National Institutes of Health, Bethesda, Maryland, USA

Bacillus anthracis **pXO1 minireplicon (MR) plasmid consisting of open reading frames (ORFs) GBAA_pXO1_0020 to GBAA_pXO1_0023 is not stably maintained in *B. anthracis*, whereas the full-size parent pXO1 plasmid (having 181,677 bp and 217 ORFs) is extremely stable under the same growth conditions. Two genetic tools developed for DNA manipulation in *B. anthracis* (Cre-*loxP* and Flp-*FRT* systems) were used to identify pXO1 regions important for plasmid stability. We localized a large segment of pXO1 that enables stable plasmid maintenance during vegetative growth. Further genetic analysis identified three genes that are necessary for pXO1 maintenance: *amsP* (GBAA_pXO1_0069), *minP* (GBAA_pXO1_0082), and *sojP* (GBAA_pXO1_0084). Analysis of conserved domains in the corresponding proteins indicated that only AmsP (activator of maintenance system of pXO1) is predicted to bind DNA, due to its strong helix-turn-helix domain. Two conserved domains were found in the MinP protein (Min protein from pXO1): an N-terminal domain having some similarity to the *B. anthracis* septum site-determining protein MinD and a C-terminal domain that resembles a baculovirus single-stranded-DNA-binding protein. The SojP protein (Soj from pXO1) contains putative Walker box motifs and belongs to the ParA family of ATPases. No sequences encoding other components of type I plasmid partition systems, namely, *cis*-acting centromere *parS* and its binding ParB protein, were identified within the pXO1 genome. A model describing the role of the MinP protein in pXO1 distribution between daughter cells is proposed.**

The large low-copy-number pXO1 plasmid (181.6 kb) of *Bacillus anthracis* encodes the anthrax toxin proteins and other virulence-related factors. Recently, we found that a pXO1 minireplicon (MR) plasmid including only open reading frames (ORFs) GBAA_pXO1_0020 to GBAA_pXO1_0023 is not stably maintained in *B. anthracis*, whereas the full-size parent pXO1 plasmid (having 181,677 bp and 217 ORFs) is extremely stable under the same growth conditions (1). (In all following text, ORF and gene names will refer to the *B. anthracis* Ames "Ancestor" strain plasmid pXO1, NCBI reference sequence NC_007322.2, and are abbreviated with retention of 3 digits, so, e.g., GBAA_pXO1_0020 is rendered as *ba020* or ORF 20). The stability of low-copy-number plasmids is typically determined by maintenance systems encoded by the plasmid. The three principal mechanistic processes that may contribute to plasmid maintenance, as described in detail by Sengupta and Austin (2), are plasmid multimer resolution, postsegregational killing of host bacteria, and plasmid partition and segregation.

Separation (or resolution) of plasmid multimers is required to maximize the number of individual plasmids available for segregation into daughter cells. Large plasmids usually contain a dedicated recombinase system consisting of a gene for a specific recombinase and a recombination site at which it acts. These site-specific recombinases resolve dimers to produce separate circular monomers suitable for partition during cell segregation. Two families of recombinases have been described for various plasmid species: active-site tyrosine recombinases and active-site serine recombinases (3).

Postsegregational killing has been described for plasmids in both Gram-negative and Gram-positive bacteria. According to this mechanism, plasmid maintenance is attributed to the presence of toxin-antitoxin loci on the plasmids that lead to killing of daughter cells that fail to receive the plasmid. These toxin-antitoxin loci are categorized into two broad classes based on the type of antitoxin: the antitoxins of type I systems are small RNAs that base-pair with the toxin mRNA to prevent protein synthesis, whereas antitoxins of type II systems are proteins that bind to and inhibit the toxin proteins (4). The recently discovered type III toxin-antitoxin systems encode protein toxins that are inhibited by pseudoknots of antitoxic RNA (5).

Plasmid partitioning is a carefully regulated process that ensures that each daughter cell receives a copy of the genetic material. Nearly all low-copy-number plasmids appear to encode a specific partition system. There are three main mechanisms for bacterial plasmid DNA partition or segregation (6): type I systems use a Walker box ATPase for plasmid partition, type II systems use actin-like ATPases, and type III systems use tubulin-like GTPases. In all cases, the systems require three components: an NTPase protein, which is thought to produce the movement required for partitioning (e.g., ParA); a partner protein, which binds to the DNA to be partitioned and regulates NTPase activity (e.g., ParB); and a *parS* centromere or region of the DNA which is bound by the partner protein. The two proteins required for partitioning are normally found encoded next to each other on the genome. The Walker A cytoskeletal P-loop ATPase system is the most common mechanism found in plasmid and chromosome segregation, and it is typified by the ParA/B system. Genes homologous to *parA* are also found outside ParA/B operons, not adjacent to a *parB*, and

Received 7 April 2014 Accepted 31 May 2014
Published ahead of print 9 June 2014
Address correspondence to Stephen H. Leppla, sleppla@niaid.nih.gov.
Supplemental material for this article may be found at http://dx.doi.org/10.1128/JB.01747-14.

doi:10.1128/JB.01747-14

these are described as being components of orphan ParA systems. Orphan ParA proteins are involved in segregating cytoplasmic proteins and protein clusters and use nonspecific chromosomal DNA binding for the segregation (7). Recently, Guynet and de la Cruz (8) presented evidence for an additional type of plasmid segregation mechanism, one not involving a plasmid-encoded motor protein and requiring only a plasmid-encoded DNA-binding protein. Plasmids with this type of segregation use the host chromosome as a carrier by an unknown mechanism.

Bacillus thuringiensis virulence plasmid pBtoxis (9) contains one of the most-studied partition systems of the large plasmids of the *Bacillus cereus* group. This plasmid has some similarities to pXO1 (1). These plasmids encode the analogous proteins TubZ and RepX, which are reported to be required for replication of pBtoxis (TubZ) and pXO1 (RepX) (10, 11). TubZ, a member of the tubulin-like GTPase superfamily, was shown to be involved along with an additional protein, TubR, in promoting stability of pBtoxis in *B. thuringiensis* (12). Ni et al. (13) showed that TubR binds to a 48-bp centromeric *tubC* site of pBtoxis and also interacts with the flexible C-terminal region of TubZ, thus attaching the TubZ filament to the plasmid, providing a mechanism for plasmid movement and, ultimately, segregation. Alternatively, Aylett and Lowe (14) identified a new *tubC* site of pBtoxis comprising seven 6-bp direct repeats. Recently, Oliva et al. (15) described a *Clostridium botulinum* lysogenic phage c-st partition system that contains all components of a type III system (TubZ, TubR, and *tubS*) along with a conserved fourth component, TubY, which modulates the TubZ-TubR-TubS complex interaction. Interestingly, several differences are found between the pBtoxis and phage c-st type III partition systems and the putative pXO1 homologs: a *tubY* homolog on pXO1 is encoded in the reverse orientation from the *repX* (*tubZ*) and *tubR* genes, unlike the parallel organization in pBtoxis, arguing against cotranscription with the other genes; low identities were found for pXO1/pBtoxis genes *tubZ* (21%), *tubR* (19%), and *tubY* (26%), while no *tubC* site (14) was identified in the pXO1 genome.

Here we describe work to localize components of the maintenance system of *B. anthracis* plasmid pXO1. Two genetic tools developed for DNA manipulation in *B. anthracis* (the Cre-*loxP* [1] and Flp-*FRT* systems) were employed to delete pXO1 regions upstream and downstream of the minireplicon. The new Flp-*FRT* recombinase method was adapted from *Saccharomyces cerevisiae* (16) and used in *B. anthracis* in a manner analogous to that of the previously described Cre-*loxP* system (1). *FRT* sites and the Flp recombinase gene were cloned into newly constructed plasmids pSCF and pFPAS, respectively. Because the two recombinases are specific for their respective *loxP* and *FRT* sites, each system can be used with target plasmids having residual sites produced by the alternative recombinase. Using these recombinases, we showed that a pXO1 region within ORFs 69 to 84 is important for plasmid maintenance. Further analysis of the region revealed three genes that are absolutely necessary for pXO1 maintenance: *ba069*, *ba082*, and *ba084*.

MATERIALS AND METHODS

Bacterial growth conditions and phenotypic characterization. *E. coli* strains were grown in Luria-Bertani (LB) broth and used as hosts for cloning. LB agar was used for selection of transformants (17). *B. anthracis* as well as *Bacillus cereus* strains were also grown in LB medium. Antibiotics (Sigma-Aldrich, St. Louis, MO) were added to the medium when appropriate to give the following final concentrations: ampicillin (Ap), 100 μg/ml (only for *Escherichia coli*); erythromycin (Em), 400 μg/ml for *E. coli* and 10 μg/ml for *B. anthracis*; spectinomycin (Sp), 150 μg/ml for both *E. coli* and *B. anthracis*; and kanamycin (Km), 20 μg/ml for *B. anthracis*. SOC medium (Quality Biologicals, Inc., Gaithersburg, MD) was used for outgrowth of transformation mixtures prior to plating on selective media to isolate transformants. *B. anthracis* spores were prepared by growth on NBY-Mn agar (nutrient broth, 8 g/liter; yeast extract, 3 g/liter; $MnSO_4 \cdot H_2O$, 25 mg/liter; agar, 15 g/liter) at 30°C for 5 days (18). Spores and vegetative cells of *B. anthracis* were visualized with a Nikon Eclipse E600W light microscope.

DNA isolation and manipulation. Preparation of plasmid DNA from *E. coli*, transformation of *E. coli*, and recombinant DNA techniques were carried out by standard procedures (17). *E. coli* SCS110 competent cells were purchased from Agilent Technologies (Santa Clara, CA) and *E. coli* TOP10 competent cells from Life Technologies (Grand Island, NY). Recombinant plasmid construction was carried out in *E. coli* TOP10. Plasmid DNA from *B. anthracis* was isolated according to the protocol for the purification of plasmid DNA from *Bacillus subtilis* (Qiagen, Germantown, MD). Chromosomal DNA from *B. anthracis* was isolated with the Wizard genomic purification kit (Promega, Madison, WI) in accordance with the protocol for isolation of genomic DNA from Gram-positive bacteria. *B. anthracis* was electroporated with unmethylated plasmid DNA isolated from *E. coli* SCS110 (lacking *dam* and *dcm*). Electroporation-competent *B. anthracis* cells were prepared and transformed as previously described (1).

Restriction enzymes, T4 ligase, T4 DNA polymerase, and alkaline phosphatase were purchased from New England BioLabs (Ipswich, MA). The pGEM-T Easy vector system (Promega) was applied for PCR fragment cloning. Phusion High-Fidelity DNA polymerase from New England BioLabs was used for the fragment PCR. Ready-To-Go PCR beads (GE Healthcare UK Limited) were used for routine DNA rearrangement analysis as described previously (1). All constructs were verified by DNA sequencing and/or restriction enzyme digestion. The oligonucleotides, plasmids, and strains used in this study are listed in Tables 1 to 3, respectively.

Marking pXO1 with a kanamycin resistance gene. To allow convenient assessment of the stability of pXO1, a kanamycin resistance cassette (Ω-km) was inserted into pXO1, replacing ORF 22 by a double-crossover event. This was accomplished by amplifying a 2,136-bp region overlapping the ORF with the 22F/22R primers and cloning the DNA into pGEM-T Easy, producing pGEM22. The 2,258-bp SmaI fragment from pUC4-ΩKM2 containing the Ω-km cassette was inserted in place of the AfeI fragment of the amplified pXO1 sequence in pGEM22, producing pGEM22Ω. The EcoRI fragment of pGEM22Ω, containing the pXO1 fragment with the internal Ω-km, was then inserted into the EcoRI site of pHY304, producing pHY304K. The Ω-km cassette from pHY304K was inserted into the homologous regions flanking ORF 22 by the double-crossover method previously described (19).

Construction of vectors for deletion analysis. Deletions in pXO1 were generated with the Cre-*loxP* system as previously described (1), employing plasmids we generically designate pSC, for *s*ingle-*c*rossover plasmid, together with pCrePAS for Cre recombinase production. We improved pCrePAS by combining the large SacI fragment of the plasmid with a SacI fragment of pUC18 (MBI Fermentas). The resulting plasmid, pCrePAS2, has permissive and restrictive temperatures of 30°C and 37°C for *B. anthracis*, respectively, and can be easily isolated from *E. coli* strains grown at 37°C. Both pSC and pCrePAS2 were used in accordance with the scheme presented in Fig. 1 of reference 1.

A new Flp-*FRT* recombinase system based on the Flp recombinase of *Saccharomyces cerevisiae* was created for use in *B. anthracis* in a manner analogous to that of the Cre-*loxP* system described previously (1). To create an analog of the pSC plasmid that we designated pSCF, we cut pHY304 (20) with Ecl136II and ligated this with a BstZ17I-restricted fragment of pMA-*FRT*, which contains a multiple-cloning site between two

TABLE 1 Oligonucleotides used in this study

Oligonucleotide	Sequence (5′–3′)[a] (location)	Relevant property	Restriction site
22F	GCAATTGAGCAATACGAACA	Primer pair to amplify pXO1 region overlapping ORF 22	
22R	AATTGTAGACATTGCGCGAC		
flpF	ACTGCATATGAGCCAGTTCGACATCCTGTGCAAGACC	Primer pair to amplify the *flp* gene	NdeI
flpR	ACTGCCCGGGAAAAGCTGGAGCTCGATATCTCATCAGATC		XmaI
190F	ACTGACTAGTCAGCTTATGGTATAGCAACG	Primer pair to amplify left fragment of ORF 29–190 deletion	XhoI
191R	ACTGCTCGAGGTCTTGGATAACCACTATCATA		SpeI
26FS	ACTGACTAGTCATTTTAATTGTTCCAGGGG	Primer pair to amplify right fragment of ORF 29–190 deletion	SpeI
29RX	ACTGCTCGAGATTGCCCGTCACTCCTTTCT		XhoI
26seqF	TCCTCATCTATCTTTTTAATTGCAGCTTCG	Primer pair to verify ORF 29–190 deletion	
190seqR	GCAGCTAACTTAGGGTCTTTCATTATTTGT		
26FX	ACTGCTCGAGCATTTTAATTGTTCCAGGGG	Primer pair to amplify left fragment of ORF 29–133 deletion	XhoI
29RS	ACTGACTAGTATTGCCCGTCACTCCTTTCT		SpeI
133F	ACTGCTCGAGGGTGTTTTTCGTTTGAAGAC	Primer pair to amplify right fragment of ORF 29–133 deletion and left fragment of ORF 137–17 deletion	XhoI
137R	ACTGACTAGTTACTTTTCGGCCTCTTCCTG		SpeI
27seqF	CTATCTTTTTAATTGCAGCT	Primer pair to verify ORF 29–133 deletion	
134seqR	ATTGTTTTCCTACAGTTTGT		
17F	ACTGCTCGAGGGCTATTTACACCAGATAAG	Primer pair to amplify right fragments of ORF 137–17, 89–17, and 79–17 deletions	XhoI
18R	ACTGACTAGTATTCTTCACAGGCTGTAAAA		SpeI
222seqF	TATTAGAATTACCACGTTCC	Primer pair to verify ORF 137–17 deletion	
18seqR1	AGATTCTTCAAAGCTATTCC		
86F	ACTGCTCGAGGTATCTGACAGAAGAAAAGAAAGAG	Primer pair to amplify left fragment of ORF 89–17 deletion	XhoI
87R	ACTGACTAGTGGATACTAGCTTCTTATATACTTGC		SpeI
87seqF	TCGACCGTATGTATCTACAC	Primer pair to verify ORF 89–17 deletion	
17seqR	CTTAATCCTTCGTTTTGTAG		
79F	ACTGCTCGAGATTTGGAGGAACAAACAATGGCTAA	Primer pair to amplify left fragment of ORF 79–17 deletion	XhoI
79R	ACTGACTAGTAAAACGTCTGGCTTTGTTTCTGGCT		SpeI
79seqF	GGCAAGTGGCGCGTATGATT	Primer pair to verify ORF 79–17 deletion	
18seqR2	GCTGAGTTGGGATGACGAAA		
80F	ACTGCGATCGGGTTGGAAAGGAACATATTA	Primer pair to amplify ORF 81–86 fragment for cloning	PvuI
87R	ACTGCGATCGCAATAACCATTGGATACATC		
84F	ACTGCTCGAGGGCAGACCTTGTTGTTCATG	Primer pair to amplify left fragment of ORF 85–19 deletion	XhoI
85R	ACTGACTAGTACAGCTGCTCTCTTTTCTTT		SpeI
19F	ACTGCTCGAGCCTTACTTCAAAAGCTGTAT	Primer pair to amplify right fragment of ORF 85–19 deletion	XhoI
19R	ACTGACTAGTGTATTTCAATGTTGCTAGGA		SpeI
85seqF	AGGAAAAACAAATCGCCTTA	Primer pair to verify ORF 85–19 deletion	
19seqR1	CCAGCCATACTATTTCACAT		
25F	ACTGCTCGAGATGGTCGTACTTGAAAATAC	Primer pair to amplify left fragment of ORF 26–68 deletion	XhoI
26R	ACTGACTAGTGCTGTTGTGTATCTTCCATA		SpeI
68F	ACTGCTCGAGTGCTCCCTCAAGTCGTGCAGTCATA	Primer pair to amplify right fragment of ORF 26–68 deletion	XhoI
69R	ACTGACTAGTCCATCGCTTAACTGCTCATCAATCA		SpeI
26seqF1	CCTTAATTCCGGATCAATCA	Primer pair to verify ORF 26–68 deletion	
68seqR	TGTACTATACGCTGAAGGTG		
83F	ACTGCTCGAGGGCTACATAAGGAGGAATAC	Primer pair to amplify left fragment of ORF 84–19 deletion	XhoI
83R	ACTGACTAGTCGAATGCTTCTCTACATAGT		SpeI
83seqF	CATTCCCGTTACTCGTTGAT	Primer pair to verify ORF 84–19 deletion	
19seqR2	CCAGCCATACTATTTCACAT		
69F	ACTGCTCGAGCGGGAAAAAATAAAAGAGAC	Primer pair to amplify right fragment of ORF 26–69 deletion	XhoI
71R	ACTGACTAGTGCGAACTATACAGTTATAGTGA		SpeI
26seqF2	AGGTGATTATAATGAACGAG	Primer pair to verify ORF 26–69 deletion	
70seqR	GTGTCCTAAGGATTTAGAAA		
68F	ACTGCGATCGGAATATACTTCCGAAGTATCGTATGTATTA	Primer pair to amplify ORF 69 and 70 fragment for cloning	PvuI
70R	ACTGCGATCGATATGGATATAGAACTGCTAAACCAAAGTT		
23F	ACTGGATATCTTTAATCCTCCACTTGTTAA	Primer pair to amplify ORF 23 downstream area for cloning	EcoRV
24R	CACGCAATGGAAATAAAATA		
81F	ATTGTAAAGATAGTTTTCGC	Primer pair to amplify fragment containing separated 67-bp stem-loop for cloning	SalI
82R	ACTGGTCGACTTTACCATTTCAAATCTCTG		
82F	ACTGGCCGGCAGAAATGATTGACATGAAAC	Primer pair to amplify fragment containing separated 45-bp stem-loop for cloning	NaeI
83R	CTTTTACAACCTGTTTGAAA		

[a] Restriction enzyme recognition sites are underlined.

TABLE 2 Plasmids used in this study

Plasmid	Relevant characteristic(s)	Source or reference
pGEM-T Easy	Cloning vector for PCR products; Ap^r in *E. coli*	Promega
pGEM22	A 2,136-bp region overlapping ORF 22 was amplified with the 22F/22R primers and cloned into pGEM-T Easy	This work
pUC4-ΩKM2	pUC4 carrying an Ω element with kanamycin resistance marker; Km^r in *E. coli* and *B. anthracis*	J. R. Scott
pGEM22Ω	A 2,258 -bp SmaI fragment from pUC4-ΩKM2 containing the Ω-km cassette was inserted instead of AfeI fragment of the amplified ORF 22 sequence in pGEM22.	This work
pHY304	Contains Em^r gene and strongly temperature-sensitive replicon for both *E. coli* and Gram-positive bacteria; Em^r in both *E. coli* and *B. anthracis*	19
pHY304K	pHY304 with pXO1 fragment containing Ω-km cassette from pGEM22Ω inserted into EcoRI; Em^r Km^r in both *E. coli* and *B. anthracis*	This work
pFLPo	Contains the Flp recombinase gene; Ap^r in *E. coli*	Addgene
pSW4	Encodes promoter of anthrax protective antigen (*pag*) in shuttle plasmid; Ap^r in *E. coli*; Km^r in *B. anthracis*	21
pSW4-Flp	pSW4 with the *flp* gene under the control of the *pagA* promoter	This work
pFPAS	Contains the entire Flp recombinase gene under the control of the *pagA* promoter; pFPAS has permissive and restrictive temperatures of 30°C and 37°C for *B. anthracis*, respectively, and can be easily isolated from *E. coli* strains grown at 37°C; Sp^r in both *E. coli* and *B. anthracis*	This work
pCrePA	pHY304 containing the entire Cre recombinase gene under the control of the *pagA* promoter	19
pCrePAS	pCrePA with Em^r replaced by Ω-sp; Sp^r in both *E. coli* and *B. anthracis*	1
pCrePAS2	pCrePAS inserted into the SacI site of pUC18. pCrePAS2 has permissive and restrictive temperatures of 30°C and 37°C for *B. anthracis*, respectively, and can be easily isolated from *E. coli* strains grown at 37°C.	This work
pSC	Contains multiple restriction site flanked by two direct *loxP* sequences; pSC has permissive and restrictive temperatures of 30°C and 37°C for *B. anthracis*, respectively. Amp^r in *E. coli*, Em^r in both *E. coli* and *B. anthracis*	1
pMA-*FRT*	Contains a multiple-cloning site between two directly repeated *FRT* sequences, ColE1origin of replication, and Amp^r gene for selection in *E. coli*	GeneArt
pSCF	pHY304 (Ecl136II) hybrid with pMA-*FRT* (*Bst*Z17I). Contains multiple restriction sites flanked by two direct *FRT* sequences; pSCF has permissive and restrictive temperatures of 30°C and 37°C for *B. anthracis*, respectively, and can be easily isolated from *E. coli* strains grown at 37°C; Amp^r in *E. coli*, Em^r in both *E. coli* and *B. anthracis*	This work
pXO1	*B. anthracis* Ames 35 plasmid	19
pXO1K	pXO1 with Ω-km cassette inserted instead of AfeI fragment of ORF 22	This work
pXO1Δ(85–19) Δ(26–68)	pXO1K with Δ(26–68) and Δ(85–19) deletions	This work
pMR	pXO1 minimal replicon; Sp^r in both *E. coli* and *B. anthracis*	1
pMR8186	ORF 81–86 PvuI fragment inserted into pMR	This work
pMR8184	pMR8186 with HpaI small fragment deleted	This work
pMR6970	pMR8184 with ORFs 69 and 70 inserted	This work
pMS10	pMR6970 with ORF 23 downstream area inserted; the UTR includes stem-loop as possible transcriptional terminator for ORF 23	This work
pMS10Δ*Bsu*36I	pMS10 with Bsu36I fragment deleted	This work
pMS10Δ*Nae*I/SalI	pMS10 with NaeI/SalI fragment deleted	This work
pMS11	pMS10 with 67-bp stem-loop deleted	This work
pMS12	pMS10 with 45-bp stem-loop deleted	This work
pMS13	pMS12 with Bsu36I/NaeI fragment deleted	This work

directly repeated *FRT* sequences, a ColE1 origin of replication, and an AmpR gene for selection in *E. coli*. The pMA-FRT plasmid was synthesized according to our design by GeneArt/Life Technologies (Grand Island, NY). The resulting pSCF provides a shuttle plasmid with all the characteristics of pSC, except that it contains repeats of the 48-bp *FRT* sequence instead of *loxP*. All of the endonuclease restriction sites located between the two direct *FRT* sequences are unique restriction sites (PvuII, XhoI, SalI, ClaI, HindIII, EcoRV, EcoRI, PstI, SmaI, BamHI, SpeI, SacII, and SacI) (see Fig. S1 in the supplemental material). To create an analog of the pCrePAS plasmid that we designated pFPAS, we purchased plasmid pFLPo from Addgene (Cambridge, MA; plasmid 13792) and amplified the *flp* gene by PCR with FlpF/FlpR primers to insert the gene into the NdeI/XmaI sites under the control of the *pagA* promoter of the pSW4 plasmid (21). The resulting pSW4-Flp plasmid was cut with BstZ17I/SnaBI. The larger BstZ17I/SnaBI fragment of pSW4-Flp containing the ColE1origin of replication, the AmpR gene for selection in *E. coli*, and the *flp* gene under the control of the *pagA* promoter was inserted into pCrePAS cut with PvuII. The resulting pFPAS plasmid provides a shuttle plasmid with all the characteristics of pCrePAS2 described in the previous paragraph but containing the *flp* gene instead of the *cre* gene.

Plasmid construction for pXO1 maintenance system search and analysis. Deletion variants of pXO1 were created *in vivo* (within *B. anthracis*) to identify regions important for plasmid maintenance. To produce the deletion [Δ(29–190)] that covers ORFs 29 to 190 (Fig. 1), we cloned two fragments amplified with primers 26FS/29RX (left fragment) and 190F/191R (right fragment) into the pSC vector; both fragments, as well as other fragments, were used according to the Cre-*loxP* system described previously (1). To produce the deletion [Δ(29–133)] that covers ORFs 29 to 133, two fragments amplified with primers 26FX/29RS (left fragment) and 133F/137R (right fragment) were cloned into pSC. Four more deletions created with the Cre-*loxP* system were located to the left (lower ORF numbers) side of the pXO1 minireplicon region: Δ(137–17) (primers 133F/137R for the left fragment and 17F/18R for the right fragment), Δ(89–17) (primers 86F/87R for the left fragment and 17F/18R for the right fragment), Δ(85–19) (primers 84F/85R for the left fragment and

TABLE 3 *B. anthracis* strains used in this study

Strain	Relevant characteristics	Reference
Ames 33	Ames pXO1$^-$ pXO2$^-$ strain	1
Ames 35	Ames pXO1$^+$ pXO2$^-$ strain	1
Ames 35S	Ames 35 with pXO1S plasmid	1
Ames 35K	Ames 35 with pXO1K plasmid	This work
Ames 35K Δ(29–190)	Ames 35K with ORFs 29–190 replaced with *loxP*	This work
Ames 35K Δ(29–133)	Ames 35K with ORFs 29–133 replaced with *loxP*	This work
Ames 35K Δ(137–17)	Ames 35K with ORFs 137–17 replaced with *loxP*	This work
Ames 35K Δ(89–17)	Ames 35K with ORFs 89–17 replaced with *loxP*	This work
Ames 35K Δ(79–17)	Ames 35K with ORFs 79–17 replaced with *loxP*	This work
Ames 35K Δ(85–19)	Ames 35K with pXO1 ORFs 85–19 replaced with *loxP*	This work
Ames 35K Δ(85–19) Δ(26–68)	Ames 35K with pXO1 ORFs 85–19 replaced with *loxP* and pXO1 ORFs 26–68 replaced with *FRT*; =Ames 33 Δ(85–19) Δ(26–68)	This work
Ames 35K Δ(84–19) Δ(26–68)	Ames 35K with pXO1 ORFs 84–19 replaced with *loxP* and pXO1 ORFs 26–68 replaced with *FRT*	This work
Ames 35K Δ(85–19) Δ(26–69)	Ames 35K with pXO1 ORFs 85–19 replaced with *loxP* and pXO1 ORFs 26–69 replaced with *FRT*	This work

19F/19R for the right fragment), and Δ(79–17) (primers 79F/79R for the left fragment and 17F/17R for the right fragment).

The newly constructed Flp-FRT system was used for deletion of an internal area of the pXO1Δ(85–19) plasmid. To produce the deletion [Δ(26–68)] that covers ORFs 26 to 68, two fragments amplified with primers 25F/26R (left fragment) and 68F/69R (right fragment) were cloned into the pSCF vector. Both fragments, as well as other fragments cloned into pSCF, were used according to Flp-FRT system described in the previous section. The FRT site replacing the deleted area was oriented clockwise in the resulting Δ(85–19) Δ(26–68) plasmid. To delete ORF 69 or ORF 84 from the Δ(85–19) Δ(26–68) plasmid, two fragments were amplified with primers 69F/71R or 83F/83R, respectively, and inserted into pSCF. In both cases, the clockwise orientation of the FRT site was saved. All deletions created with Flp-FRT system are indicated in Fig. 2A.

Direct cloning into the pMR plasmid was used to identify genes involved in pXO1 maintenance (other than ORF 69 or ORF 84). For this purpose, a fragment of 6,000 bp was amplified from pXO1 using Phusion High-Fidelity DNA polymerase (New England BioLabs, Ipswich, MA) and the 80F/87R primer pair. The fragment was inserted into the PvuI site of pMR to produce pMR8186. To eliminate ORF 85, the HpaI fragment was deleted from pMR8186 to produce pMR8184. The fragment containing ORFs 69 and 70 was amplified with the 68F/70R primer pair and inserted into the PvuI site of pMR8184 to produce pMR6970. The fragment containing both ORF 25 and a stem-loop was lost as a result of the small HpaI fragment deletion and was restored after insertion of the EcoRV/SacI fragment amplified with the 23F/24R primer pair into the single HpaI site of pMR6970. The resulting plasmid, pMS10, was cut with either Bsu36I or NaeI/SalI. The sticky ends were filled with corresponding deoxynucleotides by T4 polymerase according to the New England BioLabs protocol for blunting ends by the filling in of 5′ overhangs. The blunt ends of each fragment containing the pXO1 minireplicon were ligated to produce either pMS10Δ*Bsu*36I or pMS10ΔNaeI/SalI. To produce pMS11 and pMS12, the small NaeI/SalI fragment of pMS10 was replaced with either the NaeI/SalI fragment of the PCR product amplified with 82F/83R primers (pMS11) or the NaeI/SalI fragment of the PCR product amplified with 81F/82R primers (pMS12). To produce pMS13, the Bsu36I/NaeI fragment of pMS12 was deleted.

Segregational stability assay. Plasmid pXO1 has a copy number of approximately three (22, 23), so the short (27-min) doubling time of the bacteria leads to rapid loss of pXO1 in the absence of a partition system. The stabilities of pXO1 and its Km^r derivatives were determined using methods described previously (1), with slight modification. The *B. anthracis* strains containing plasmids were grown on LB agar with the corresponding antibiotic to obtain separated colonies. The separated colonies were spread on LB agar as a strip (approximately 3 by 20 mm). Twelve passages on nonselective LB agar were performed from the strips at 12-h intervals. After each passage, bacteria were diluted in phosphate-buffered saline (Quality Biologicals, Inc., Gaithersburg, MD) and titrated, and aliquots were plated on agar with and without antibiotic to determine the percentage of cells retaining the plasmid.

DNA sequencing and protein bioinformatic analyses. Plasmid DNAs were sequenced using primers listed in Table 1. Primers for sequencing were synthesized by Integrated DNA Technologies, Inc., Coralville, IA. Sequences were determined using a primer walking strategy (Macrogen, Rockville, MD). Sequence data were assembled using either the Clustal module of the GCG-Lite suite of sequence analysis program (http://helixweb.nih.gov/emboss-lite/) or Vector NTI software (Invitrogen). The National Center for Biotechnology Information (NCBI) BLAST and FASTA programs (http://www.ncbi.nlm.nih.gov) were used for homology searches in GenBank and nonredundant protein sequence databases. The Pfam database (http://pfam.sanger.ac.uk) was used for alignment to ORF 82. Repeat Finder and RepeatAround (24) software was used to locate direct repeats (DRs) and inverted repeats (IRs). Predicted protein motifs were analyzed using SignalP software version 3.0 for prediction of signal sequences (http://www.cbs.dtu.dk/services/SignalP), TMpred software for prediction of transmembrane regions and orientation (http://www.ch.embnet.org/software/TMPRED_form.html), NPS@ software (http://npsa-pbil.ibcp.fr) for helix-turn-helix (H-T-H) prediction, and Meta-Server for protein domain searches (http://prodata.swmed.edu/MESSA/).

RESULTS

Cre-*loxP*-generated deletions identify pXO1 regions responsible for plasmid maintenance. The Cre-*loxP* system was used to create a number of large deletions of various regions of pXO1 (Fig. 1A). The largest deletion removed genes corresponding to ORFs 29 to 190 [Δ(29–190)]. This region includes two prominent features, a putative type III plasmid partition system (PPS; ORFs 67 to 69) and a region designated a pathogenicity island (PAI; ORFs 131 to 194) (Fig. 1A and B). The PPS contains the *tubZ-tubR-tubY* gene cluster, whereas the PAI contains the anthrax toxin genes within a 44.8-kb segment defined by terminal inverted IS*1627* elements. The PAI is inverted in some strains (18, 25, 26). Confirmation of this deletion (along with other deletions created by the Cre-*loxP* system) is provided in Fig. 1C, which shows the results of a PCR that was performed with primers flanking the deleted regions. Sequencing the PCR products confirmed replacement of the deleted areas with the *loxP* site (data not shown). The Ames 35K Δ(29–190) strain containing pXO1 with this deletion lost this

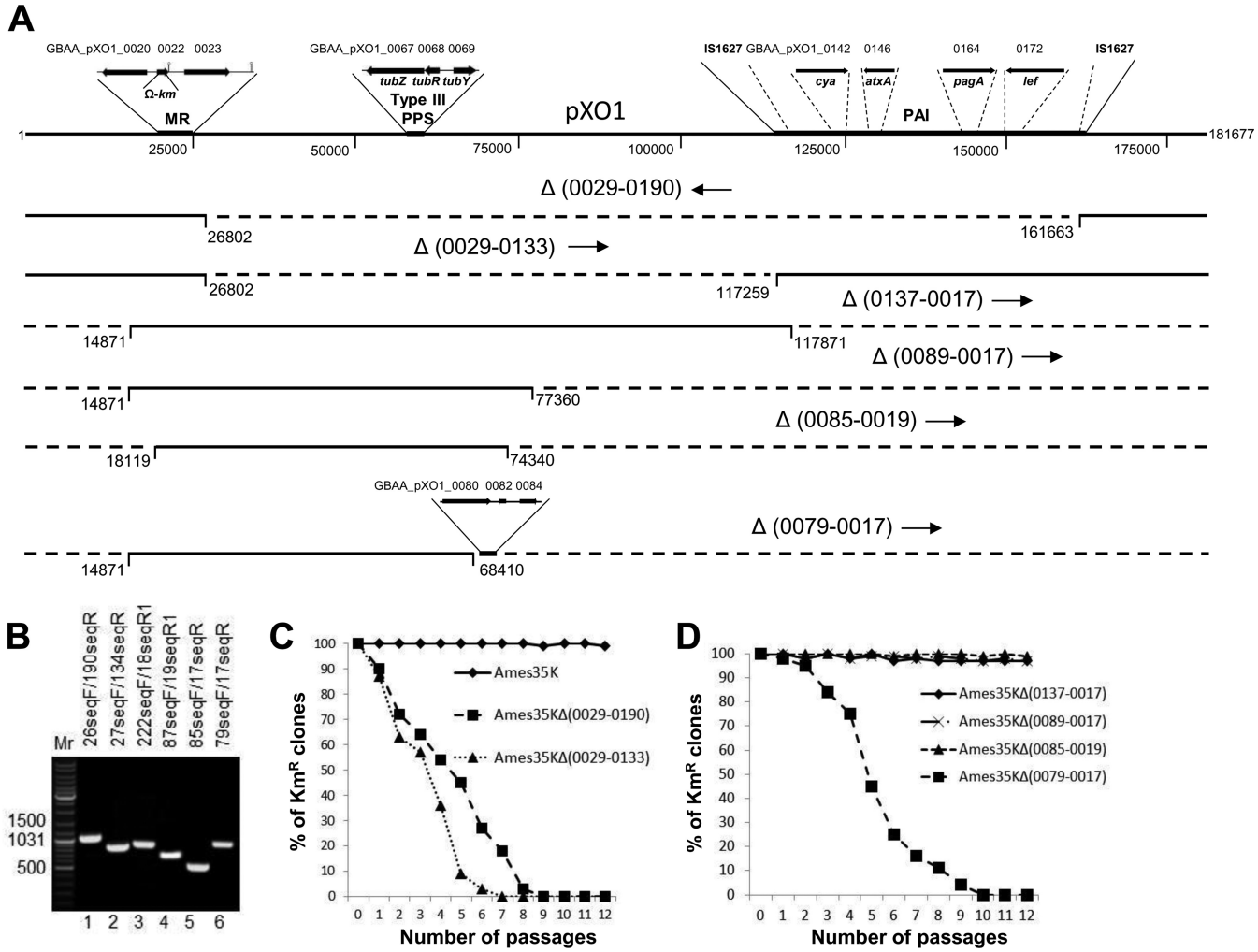

FIG 1 Effects of large deletions within pXO1 on plasmid stability. (A) The pXO1 structure with the minireplicon (MR), type III plasmid partition system (type III PPS), and pathogenicity island (PAI) indicated. The MR structure is adopted from reference 1 and shown with the Ω-km cassette inserted into pXO1 GBAA_pXO1_0022 to produce pXO1K. The type III PPS structure is adopted from reference 15 and includes the newly described *tubY* gene, important for functionality of the type III PPS. The PAI structure with indication of IS*1627* insertion sequences and *B. anthracis* toxin components was prepared according to the complete sequence of Ames Ancestor plasmid pXO1 (NCBI reference sequence NC_007322.2). The numbers located below and on both sides of pXO1 represent nucleotide numbers in the complete sequence. The GBAA_pXO1_ symbols along the top of pXO1 and along the bottom line are locus tag numbers for the Ames Ancestor plasmid pXO1. The pXO1 regions deleted in each construct are shown in parentheses following the Greek letter delta (the numbers are for the ORFs of the area deleted). Orientations of *loxP* sites that replaced the deleted region are indicated by arrows. The numbers located below the deletions (dashed lines) are the first and last base pairs included in the deletions. (B) PCR verification of the deletions. Primers used to verify retention of specific segments are indicated at the top of the gel. Lanes: 1, Ames 35K Δ(29–190); 2, Ames 35K Δ(29–133); 3, Ames 35K Δ(137–17); 4, Ames 35K Δ(89–17); 5, Ames 35K Δ(85–19); and 6, Ames 35K Δ(79–17). Mr is a GeneRuler DNA ladder mix for size determination (e.g., 1,500 bp). (C) Percentage of kanamycin-resistant (i.e., plasmid-containing) bacteria in cultures of *B. anthracis* Ames 35 containing either pXO1K or pXO1K with deletions produced in pXO1. Bacteria were subcultured every 12 h on LB agar without kanamycin and grown at 37°C. Bacteria from each subculture were diluted and plated on LB agar with and without kanamycin (20 μg/ml) to determine the fraction retaining the plasmids. Maximum root mean square deviations in the percentage of kanamycin-resistant colonies did not exceed 10%. (D) Percentage of kanamycin-resistant (i.e., plasmid-containing) bacteria in cultures of *B. anthracis* Ames 35 containing pXO1K with deletions extending clockwise around the circular plasmid from bp 181677 (and ORF 217) past bp 1. Maximum root mean square deviations in the percentage of kanamycin-resistant colonies did not exceed 10%.

plasmid upon repeated passage (Fig. 1D), indicating that the deleted region contained at least one gene or sequence important for pXO1 stability.

The next large pXO1 deletion, which removed ORFs 29 to 133 [Δ(29–133)], also greatly decreased plasmid stability (Fig. 1D), indicating that the deleted region is important for stability, consistent with a requirement for the type III PPS genes. This suggestion was supported by the behavior of the Δ(137–17) strain, which is almost the complement of the Δ(29–133) strain (Fig. 1B). The Δ(137–17) strain contained the type III PPS genes and was stably maintained (Fig. 1E). Several subsequent deletions indicated in Fig. 1B resulted in strain Ames 35K Δ(85–19), which stably maintained the corresponding deletion mutant plasmid during 12 passages on media without kanamycin. The final deletion indicated in Fig. 1B produced strain Ames 35K Δ(79–17), which rapidly lost the pXO1Δ(79–17) variant although the type III PPS was present (Fig. 1E). This observation led us to conclude that features important for pXO1 maintenance are located within the area of ORFs 80 to 84.

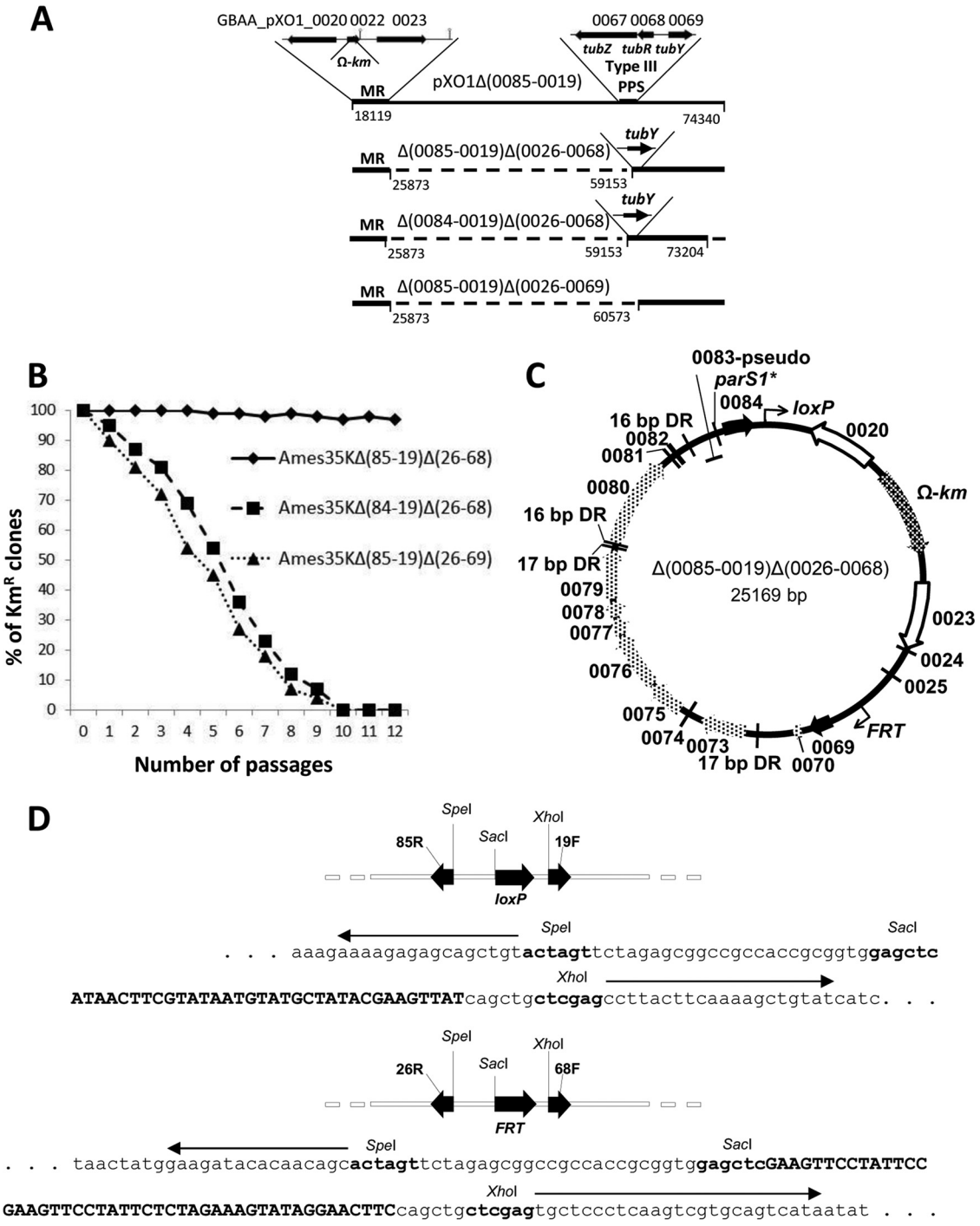

FIG 2 Deletions created with Cre and Flp identify ORFs 69 and 84 as being important for plasmid stability. (A) Deletions produced by the Flp-*FRT* system within pXO1Δ(85–19) resulted in pXO1Δ(85–19) Δ(26–68), which retained plasmid stability. Deletion of either GBAA_pXO1_0084 or GBAA_pXO1_0069 decreased stability of pXO1Δ(85–19) Δ(26–68), which we redesignate circular Δ(0085–0019) Δ(0026–0068) (see panel C). (B) Percentages of kanamycin-resistant (i.e., plasmid-containing) bacteria in cultures of *B. anthracis* Ames 35 containing either Δ(0085–0019) Δ(0026–0068) plasmid or the plasmids with single flanking genes deleted were determined as described in Materials and Methods. (C) Genetic map of the mini-pXO1 plasmid Δ(0085–0019) Δ(0026–0068). ORFs of the pXO1 minireplicon (MR) are indicated with unfilled arrows, ORFs important for maintenance are indicated with black arrows, and additional predicted ORFs are indicated with light patterned arrows. The Ω-km cassette is located within the minireplicon and is indicated with a dark patterned arrow. The 16- and 17-bp direct repeats are labeled as DRs. The *loxP* and *FRT* sites generated during the deletion events are indicated as bent arrows. The putative centromere *parS1** located between the GBAA_pXO1_0083 pseudogene and the GBAA_pXO1_0084 gene is indicated as an arc. (D) Graphic representation of the deletion junction sites for the Δ(0085–0019) Δ(0026–0068) plasmid. The *loxP* site is shown in the upper portion along with the sequence indicating the *loxP* site within the Δ(0085–0019) Δ(0026–0068) junction site. Arrows indicate 85R and 19F primers; endonuclease restriction sites are shown in bold, and *loxP* is shown in bold uppercase. The *FRT* site is shown in the bottom portion along with the sequence indicating the *FRT* site within the Δ(0085–0019) Δ(0026–0068) junction site. Arrows indicate 26R and 68F primers; endonuclease restriction sites are shown in bold, and *FRT* is shown in bold uppercase.

To determine whether the five-ORF region just described is sufficient to confer stability, we cloned into pMR a fragment extending from the end of ORF 80 to the end of ORF 87. The resulting plasmid, pMR8186 (described more fully in Fig. 3), was used to transform the Ames 33 strain, and the stability of the plasmid was compared with that of pMR. The pMR8186 plasmid had the same low stability as the pMR plasmid (data not shown). This demonstrated that the cloned region does not contain the entire maintenance system, and plasmid maintenance requires additional factors located elsewhere on pXO1, probably in the area between ORFs 23 and 79. Because not all plasmids containing a *loxP* site can be further deleted in a controlled manner by the Cre-*loxP* approach, we developed a parallel system for doing deletions using the Flp recombinase, as described in Materials and Methods.

Sequential Cre-*loxP*- and Flp-*FRT*-generated deletions identify two noncontiguous pXO1 genes important for plasmid maintenance. Results from sequential Cre-*loxP*- and Flp-*FRT*-generated deletions are shown in Fig. 2A. Primer pairs 25F/26R and 68F/69R were used for amplification of fragments used to produce an internal deletion in pXO1Δ(85–19) that included ORFs 26 to 68. The resulting plasmid, pXO1Δ(85–19) Δ(26–68), was retained upon repeated passage (Fig. 2B), showing it retained all components important for plasmid partition. A physical map of the plasmid pXO1Δ(85–19) Δ(26–68) is shown in Fig. 2C, and nucleotide sequences of the single *loxP* and *FRT* sites within the plasmid were confirmed as shown in Fig. 2D.

To identify regions of pXO1Δ(85–19) Δ(26–68) needed for maintenance, additional deletions were created and analyzed. Extending the large deletion to include an additional gene at each end, either *ba069* or *ba084* (Fig. 2A), greatly decreased plasmid stability (Fig. 2B). This key result showed that the DNA segments corresponding to ORFs 69 and 84 are important for plasmid stability.

Inferences regarding the roles of ORFs 69 and 84 were made by sequence comparisons. Analysis of conserved domains in ORF 84 (http://www.ncbi.nlm.nih.gov) indicated that the protein resembles the *B. subtilis* Soj protein, a defining member of the ParA family of ATPases involved in plasmid/chromosome partitioning. This protein contains a putative Walker box, indicating its possible role in pXO1 partitioning. Analysis of ORF 69 predicts that it is a DNA-binding protein, one with a strong H-T-H motif. The presence of the H-T-H motif indicates that this protein could play the role of ParB in pXO1 partitioning. The current annotation of ORF 69 as encoding a transcriptional regulator belonging to the MerR superfamily, rather than as a ParB family member, probably derives from its putative DNA-binding activity. It is interesting that all other proteins encoded within the area from ORFs 69 to 84 of the *B. anthracis* Ames Ancestor strain plasmid pXO1 (NCBI reference sequence NC_007322.2) are annotated only as hypothetical proteins, with the exception of the ORF 79 protein, which is identified as a "surface layer protein."

Sequence analyses to search for candidate DNA elements important for plasmid partition. Type I partition systems typically include a centromere-like *parS1* site. It is interesting that a possible *parS1** (asterisk indicates an imperfect *parS1* palindrome) site is located 136 bp upstream of ORF 84 (Fig. 2C). This site is imperfect in having two discrepancies from the consensus *parS1* (27), specifically C instead of G in position 9 and transversion of AC in positions 13 and 14: TGTTTCACCTGAACAA (*parS1**) versus TGTTTCACGTGAAACA (*parS1*). We also searched upstream of ORF 84 for adjacent direct repeats (DRs) that could play the role of alternative *cis*-acting centromere sites (28). While no adjacent DRs were found, there are noncontiguous DRs of 16 bp (AGGTG TGTCCTTTTTT) and 17 bp (ATATAATATAAAAATAA) within ORFs 69 to 84. The 16-bp DRs flank the region from ORFs 80 to 82, and the 17-bp DRs flank the region from ORFs 72 to 79, as shown in Fig. 2C.

Creation of a small, stable recombinant plasmid. While the deletion analyses described above identified ORFs 69 and 84 as important for maintenance, they did not exclude that additional factors are required. To facilitate analysis of the region between these two genes, we directly cloned several fragments into a pMR plasmid to assess their roles. This cloning began with plasmid pMR8186, mentioned above, which contains pMR connected with the segment from ORFs 81 to 87 (Fig. 3A). First, we deleted the HpaI fragment containing ORFs 85 to 87 along with the essential stem-loop of the minireplicon (see Fig. 4 of reference 1). The resulting plasmid, pMR8184, therefore lost the ability to transform *B. anthracis* due to the loss of the minireplicon function. The unique PvuI site to the left of ORF 83 of the pMR8184 plasmid was used for the insertion of a PvuI fragment amplified with the 68F/69R primer pair so as to contain ORFs 69 and 70. Subsequently, the unique HpaI site of the resulting pMR6984 plasmid (not shown) was used for insertion of an EcoRV/SacI fragment amplified from pMR with the 23F/24R primer pair. The final pMS10 construct (Fig. 3A) contained ORFs 69 and 70, ORFs 81 to 85, and the restored minireplicon region. A plasmid stability test demonstrated that pMS10 is stably maintained in *B. anthracis* cells (Fig. 3B).

To further define the role of the pMS10 internal region including ORFs 70 to 83, we separately deleted the Bsu36I and NaeI/SalI fragments from the pMS internal region. Both resulting plasmids, pMS10Δ *Bsu*36I and pMS10Δ *Nae*I/SalI, lost stability in *B. anthracis* Ames 33 (Fig. 3B). Because the two deletions overlap at ORFs 81 and 82, we analyzed this region further.

ORF 82 is important for pMS10 stability. We noted stem-loop structures (SLS) of 67 bp and 45 bp in the region of ORFs 81 and 82 and considered whether they might play a role (Fig. 4A). The larger SLS is located within ORF 82 and the smaller in the intergenic region between ORFs 82 and 83. The 45-bp SLS contains an internal Bsu36I site. To delete each of the SLS separately, we cut out the pMS10 NaeI/SalI fragment and replaced it with fragments containing either the 67-bp or the 45-bp SLS, as described in Materials and Methods (Fig. 4A). The resulting pMS11 and pMS12 plasmids were electroporated into *B. anthracis* strain Ames 33, in which it was found that the pMS12 plasmid was completely retained in *B. anthracis* during 12 passages without selective pressure, while pMS11 was lost under the same conditions (Fig. 4B). This result demonstrated that the region from ORFs 70 to 81 is not sufficient to maintain these pMS plasmids in *B. anthracis*. Furthermore, the 45-bp SLS and ORF 83 pseudogene are not necessary for plasmid stability. On the other hand, the ORF 82 region is important to retain pMS10 in *B. anthracis* cells.

It is interesting that *ba082* contains five transcriptional start sites (Fig. 5A) and is located between two large operons that are transcribed in the orientation opposite that of this gene (29). We also found a putative σ^A-dependent promoter located upstream of ORF 82 and two additional translational start codons encoded in the same reading frame as the start codon identified in the Ames

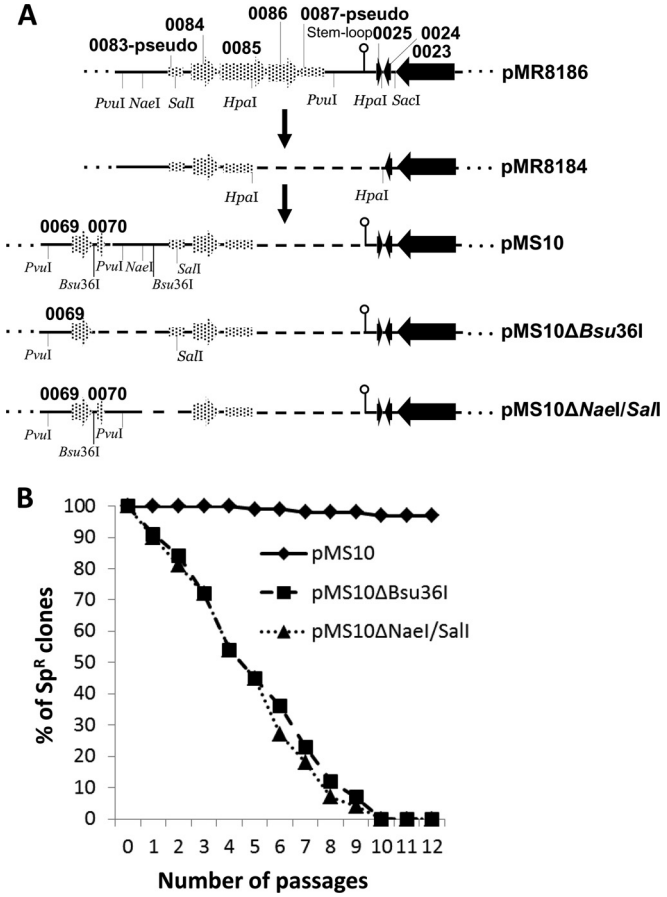

FIG 3 Creation and stability analysis of pMS10. (A) Deletion of the pMR8186 HpaI fragment resulted in pMR8184, which lost the ability to transform *B. anthracis* Ames 33. Supplementation of pMR8184 with the GBAA_pXO1_0069–0070 region and GBAA_pXO1_0025 along with the downstream stem-loop restored the transformation ability of the resulting plasmid pMS10. Deletion of either the Bsu36I or NaeI/SalI fragment of pMS10 produced the unstable plasmids diagramed here. (B) Percentage of spectinomycin-resistant (i.e., plasmid-containing) bacteria in cultures of *B. anthracis* Ames 33 containing either pMS10 or pMS10 with the Bsu36I or NaeI/SalI fragment deleted. Cultures were subcultured every 12 h on LB agar without spectinomycin and grown at 37°C. Bacteria from each subculture were diluted and plated on LB agar with and without spectinomycin (150 μg/ml) to see the fraction retaining the plasmids. Maximum root mean square deviations in the percentage of spectinomycin-resistant colonies did not exceed 10%.

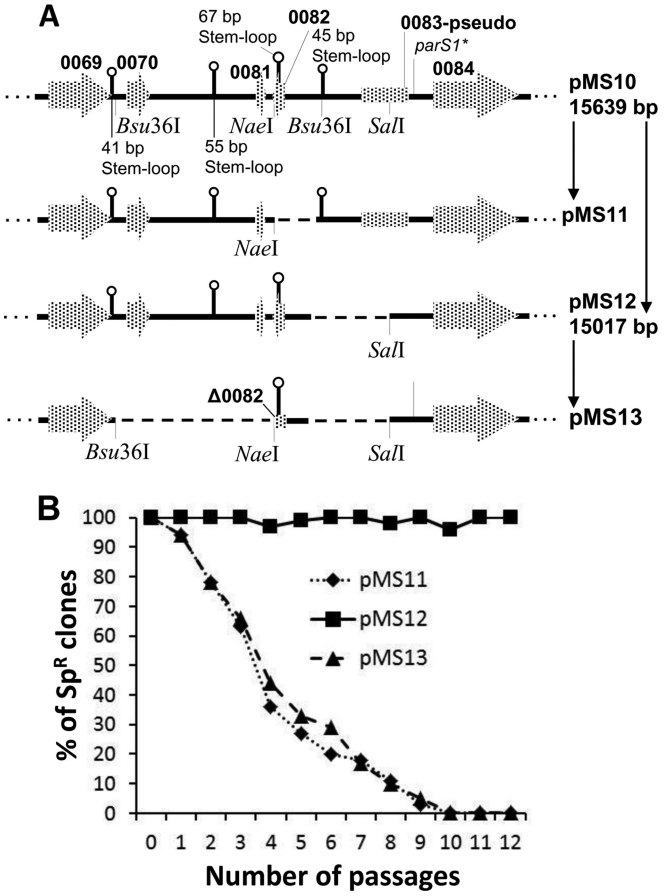

FIG 4 Search for regions involved in stability of pMS10. (A) Construction of the pMS10 deletions. Two stem-loops of 67 and 45 bp were found within pMS10 NaeI/Bsu36I fragment. Deletion of the 67-bp stem-loop resulted in pMS11, while deletion of the 45-bp stem-loop resulted in pMS12. Deletion of the pMS10 Bsu36I/NaeI fragment of pMS12 resulted in pMS13. Two more stem-loops of loops 41 and 55 bp are shown on the plasmid map. These are potential transcriptional terminators for GBAA_pXO1_0069 and GBAA_pXO1_0080, respectively (ORF 80 was deleted during pMR8186 creation). (B) Percentage of spectinomycin-resistant (i.e., plasmid-containing) bacteria in cultures of *B. anthracis* Ames 33 containing either pMS111, pMS122, or pMS13 were determined as described previously.

Ancestor plasmid pXO1 annotation (NCBI reference sequence NC_007322.2). The variety of transcriptional and translational start sites could be indicative of a complex pattern of *ba082* regulation.

To clarify the role of ORF 82 in pXO1 maintenance, we analyzed the sequence of the corresponding hypothetical protein (76 amino acids [aa]) using MESSA software (30). Two conserved domains were found in the protein sequence (Fig. 5B). The N-terminal part of the sequence (aa 9 to 47) resembles the *B. anthracis* septum site-determining protein MinD, with 13 of 42 residues being identical and 23 being either identical or of a similar type. The C-terminal part of the 76-aa protein (aa 55 to 74) resembles a highly basic, single-stranded DNA (ssDNA)-binding protein from a family of baculovirus ssDNA-binding proteins, with 9 of 24 residues being identical and 13 being either identical or of a similar type. The protein is well conserved in plasmids of the *B. cereus* group (*B. anthracis*, *B. cereus*, and *B. thuringiensis*), with key residues of both domains being conserved (Fig. 5C).

The deletion analysis described above could not determine whether the *ba082* DNA segment functioned as a DNA target, an mRNA, or a translated polypeptide. To address this, we deleted the pMS12 Bsu36I/NaeI fragment (Fig. 4A), thereby truncating the putative protein by 11 amino acids while retaining the 67-bp SLS. The stability test demonstrated that the resulting pMS13 plasmid lost stability in comparison with pMS12. This result argues against the 67-bp SLS having a role as a centromere bound by the ORF 69 protein.

DISCUSSION

In the present study, we identified three noncontiguous genes on the pXO1 plasmid that are sufficient for stable maintenance of mini-pXO1 plasmids created *in vivo* or recombinant pXO1-derived mini-replicon plasmids containing the previously identified replication

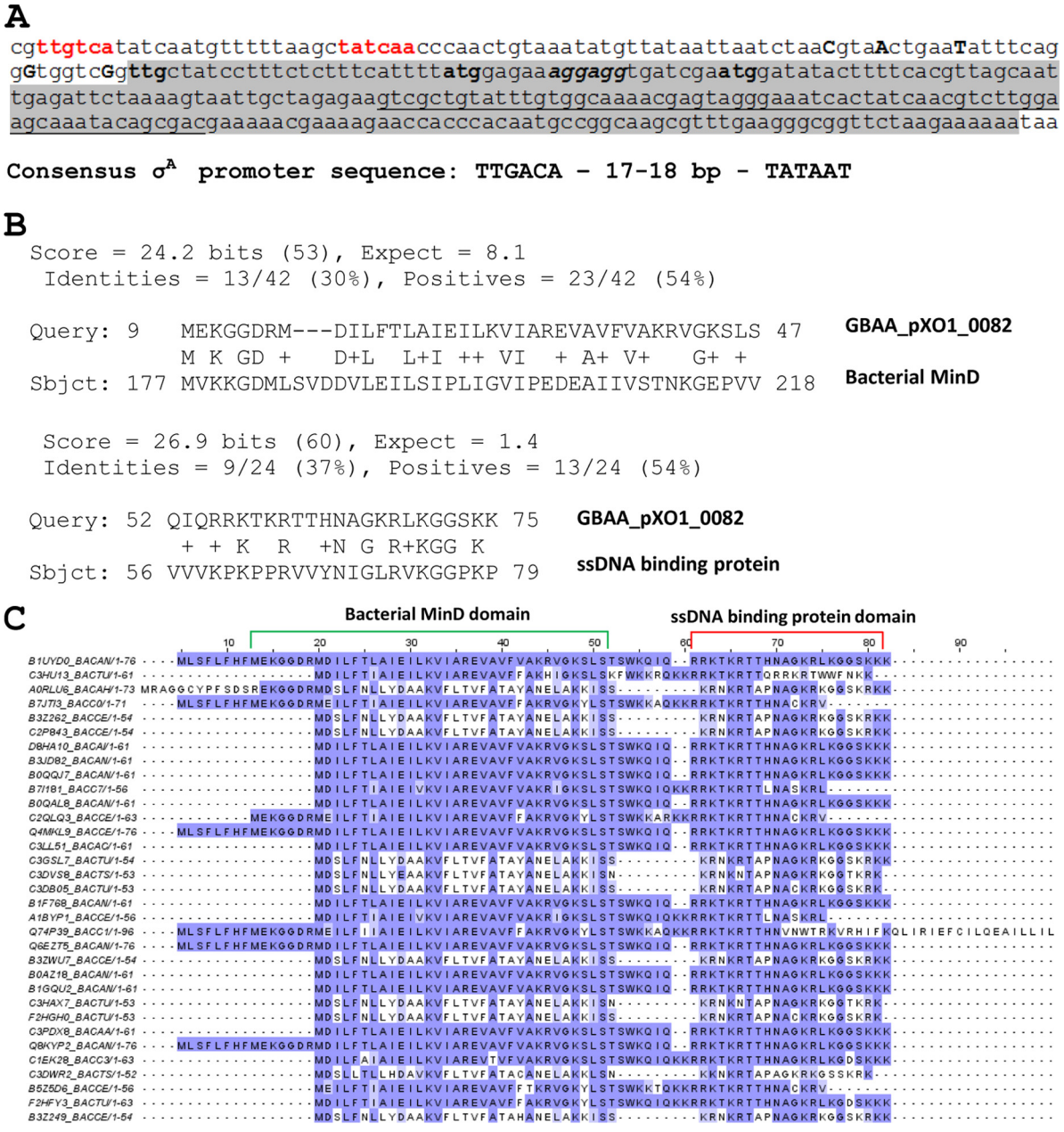

FIG 5 Nucleotide sequence of *minP* gene and amino acid sequence of MinP protein in comparison with cognate proteins from *B. cereus* group. (A) *minP* nucleotide sequence. The −35 and −10 regions of the σ^A-like promoter are indicated in red. Five transcriptional start sites identified by transcriptome sequencing (RNA-seq) (29) are shown in uppercase with bold. The structural part of the gene is shaded. Three potential translation start codons are shown in bold, while the consensus Shine-Dalgarno sequence is in italics with bold. The 67-bp stem-loop is underlined. (B) Alignment of MinP using Meta-Server for protein domain searches (http://prodata.swmed.edu/MESSA/). (C) MinP alignment. The Pfam protein database was used to align proteins. The top row shows the Ames Ancestor pXO1 MinP amino acid sequence. Amino acids matching the top reference sequence are indicated in dark violet. Amino acids with similarity to the reference are shown in light violet. The bacterial MinD domain and the ssDNA-binding protein domain are indicated by green and red brackets, respectively.

genes (1). We named the three corresponding proteins according to their predicted functions in plasmid maintenance: AmsP (activator of maintenance system of pXO1; corresponds to ORF 69), MinP (plasmid-encoded Min protein; corresponds to ORF 82), and SojP (plasmid-encoded Soj; corresponds to ORF 84).

AmsP is similar to the TubY protein, which is a component of the previously described pBtoxis type III PPS (15). However, the established pXO1 maintenance system did not require the two other pXO1 proteins that correspond to the TubZ and TubR proteins of the pBtoxis PPS. This was evident from the continued stability of the pXO1Δ(85–19) Δ(26–68), pMS10, and pMS12 plasmids (Fig. 2 to 4), in which the TubZ and TubR homologs were deleted. Also, in contrast to pBtoxis, transcription of the *amsP* gene in pXO1 is oriented in the direction opposite that of the *tubZ* and *tubR* homologs, whereas in pBtoxis all three *tub* genes are within a single operon.

The analysis and data described above demonstrated that a classical type III PPS (12) like that in pBtoxis is not sufficient for optimal stability of plasmids, as illustrated by the instability of the pXO1Δ(79–17) derivative plasmid (Fig. 1). This led us to search for proteins resembling those in the type I and type II PPSs. We correlated SojP with the ParA protein of the type I PPS because this protein belongs to Walker-type ATPases from the ParA family (http://www.ncbi.nlm.nih.gov; http://prodata.swmed.edu/MESSA/). Also, the gene encoding this protein contains an upstream *parS1** sequence similar to *parS1* (Fig. 2). Accordingly, the presence of a DNA-binding motif within the AmsP protein could designate this protein not only as a transcriptional activator but also as an analog of ParB (6). In this case, we could interpret AmsP and SojP as proteins belonging to the type I PPS.

However, in contrast to the classical type I system represented by a *parAB* operon, the genes encoding the proteins responsible for the pXO1 partition are split and divided. It was interesting to find two sets of DRs (16 and 17 bp in length) flanking the area dividing ORF 69 (i.e., *parB*) and ORF 84 (i.e., *parA*) (Fig. 2C). Both DR sets could have served as recombinase targets during evolutionary events that disrupted an ancestral *parAB* operon. Additional evidence for an ancestral *parAB* operon is the presence of the imperfect centromere *parS1** that is located immediately next to the start of ORF 84 (i.e., *parA*). It is remarkable that a chromosomal *parS1* sequence is located at position 218403 to 218418 in the *B. anthracis* Ames Ancestor, between GBAA_0228 and GBAA_0229, which are transcribed from opposite DNA strands. However, the chromosomal *parAB* gene cluster is located far away from this area: *parA* (i.e., *soj*, GBAA_5730) is at position 7598 to 8359 and *parB* (i.e., *spo0J*) is at position 8433 to 9203. An additional *parB* (i.e., *spo0J*, GBAA_5729) is upstream of the *parA* region. The presence of so many discrepancies within a supposed type I PPS suggests that this system may not be active in either pXO1 or chromosomal DNA partitioning.

What kind of plasmid segregation system consistent with the data presented above could explain pXO1 partitioning? Upon accepting AmsP as a transcriptional activator, we concentrated on the MinP (i.e., Min protein) and SojP (i.e., ParA) proteins. These proteins belong to the ParA/MinD family recently described by Lutkenhaus (31). In accordance with his model, in many bacteria the MinD protein is involved in spatial regulation of the cytokinetic Z ring, and ParA proteins are involved in chromosome and plasmid segregation. The Min system in *B. subtilis* (the closest to *B. anthracis* of the well-studied bacterial species) uses the DivIVA protein to recruit the Min proteins. The DivIVA protein forms a ring on either side of the invaginating septum and recruits MinJ, which recruits MinD, which recruits MinC (32, 33). Both rings maintain their diameter as septation proceeds at the junction of the dividing cells, but once cells separate, the pole takes on a hemispherical shape and DivIVA is remodeled (34). The Min proteins are eventually released and are able to join DivIVA, assembling at the next incipient division site.

The *B. anthracis* Ames Ancestor (NCBI reference sequence NC_007530.2) chromosomal DNA encodes all components of this machinery: cell division protein FtsZ (GBAA_4045), the polarity determinant DivIVA (GBAA_1583, indicated as a hypothetical protein), MinC (GBAA_4681, indicated as a septum formation inhibitor), MinD (GBAA_4680, indicated as the septum site-determining MinD protein), and GBAA_5412, encoding a protein that has 36% identity and 60% positivity with *B. subtilis* cell division topological determinant MinJ. It is interesting that DivIVA might interact with the MinJ transmembrane domain and that MinD might interact with the MinJ PDZ domain (32, 33). In either scenario, the two halves of MinJ could interact with MinD and DivIVA, respectively, to sequester membrane-bound MinD to the poles of the cell (31).

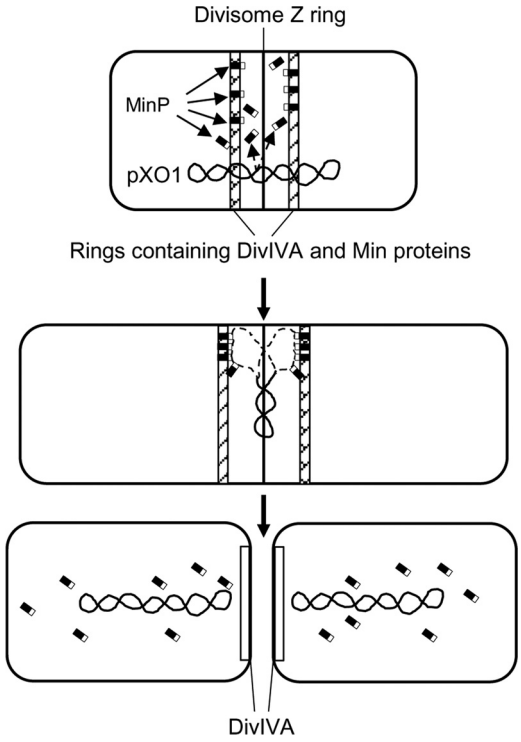

FIG 6 Model for pXO1 distribution between incipient cells by MinP protein. (Top) The divisome Z ring is flanked by two rings containing DivIVA and Min proteins, modeled after reference 31. The N-terminal part of the MinP protein (indicated as black area in MinP rectangle) is intercalated into the flanking rings. (Middle) Two DNA single-strand loops (indicated by dashed lines) generated during pXO1 replication interact with the C-terminal part of MinP protein (indicated as white area in MinP rectangle). (Bottom) Two pXO1 copies fixed on different rings move to the adjusted poles of dividing cells and, after the cells divide, are released. MinP and other Min proteins leave the rings, and DivIVA reorganizes.

In considering how these proteins may function in pXO1 partitioning, we suggest that the N-terminal part of MinP is involved in interaction with the rest of the proteins of the Min-DivIVA complex. Theoretically, we can make this suggestion according to MinP and MinD, MinC sequences similarity. Since the C-terminal part of the MinP protein containing the putative ssDNA-binding domain could associate with each strand of the replicating pXO1, it is possible that the two Min-DivIVA rings each distribute a pXO1 copy into the compartments divided by the *B. anthracis* divisome. The structure and properties of the *B. anthracis* divisome are unknown, but the *B. subtilis* divisome can be used as a model of what may exist in *B. anthracis* (35).

Structural analysis of the SojP protein using MESSA software (30) showed that SojP is similar to MinD of *B. anthracis* Ames Ancestor (GBAA_4680) and to MinD of several other bacteria. This is not surprising, because the structures of all MinD and ParA proteins show a high degree of similarity (36). Consequently, the N-terminal domain of SojP (i.e., *parA*) could be a part of the

Min-DivIVA rings and the C-terminal domain could be used for non-sequence-specific DNA-binding activity for either chromosomal or pXO1 double-stranded DNA (36).

When pXO1 replication is finished, pXO1-SojP, along with the Min proteins, could be used as a motor to localize Min-DivIVA proteins and pXO1 plasmid copies to the poles of divided cells. The role of SojP could be interpreted as an orphan ParA using nonspecific DNA binding for segregation without involvement of *parS* and ParB homologs (7). However, how pXO1-SojP may participate in this localization is unclear. After the cells divide, Min proteins are released and DivIVA is reorganized (31). A model of pXO1 partitioning, along with *B. anthracis* cell division, is presented in Fig. 6. To evaluate the validity of this model, it will be useful to search for MinP interactions with the DivIVA, MinJ, MinD, and MinC proteins forming the rings flanking the divisome and to assess the affinity of MinP for single-stranded pXO1. The detailed description of these interactions demands further study of specific protein-protein and DNA-protein contacts.

ACKNOWLEDGMENTS

This research was supported by the Intramural Research Program of the NIH National Institute of Allergy and Infectious Diseases.

We thank June R. Scott (Department of Microbiology and Immunology, Emory University School of Medicine, Atlanta, GA) for plasmid pUC4-ΩKM2.

REFERENCES

1. **Pomerantsev AP, Camp A, Leppla SH.** 2009. A new minimal replicon of *Bacillus anthracis* plasmid pXO1. J. Bacteriol. **191:**5134–5146. http://dx.doi.org/10.1128/JB.00422-09.
2. **Sengupta M, Austin S.** 2011. Prevalence and significance of plasmid maintenance functions in the virulence plasmids of pathogenic bacteria. Infect. Immun. **79:**2502–2509. http://dx.doi.org/10.1128/IAI.00127-11.
3. **Stark WM, Boocock MR, Sherratt DJ.** 1992. Catalysis by site-specific recombinases. Trends Genet. **8:**432–439. http://dx.doi.org/10.1016/0168-9525(92)90327-Z.
4. **Fozo EM, Makarova KS, Shabalina SA, Yutin N, Koonin EV, Storz G.** 2010. Abundance of type I toxin-antitoxin systems in bacteria: searches for new candidates and discovery of novel families. Nucleic Acids Res. **38:**3743–3759. http://dx.doi.org/10.1093/nar/gkq054.
5. **Blower TR, Short FL, Rao F, Mizuguchi K, Pei XY, Fineran PC, Luisi BF, Salmond GP.** 2012. Identification and classification of bacterial type III toxin-antitoxin systems encoded in chromosomal and plasmid genomes. Nucleic Acids Res. **40:**6158–6173. http://dx.doi.org/10.1093/nar/gks231.
6. **Gerdes K, Howard M, Szardenings F.** 2010. Pushing and pulling in prokaryotic DNA segregation. Cell **141:**927–942. http://dx.doi.org/10.1016/j.cell.2010.05.033.
7. **Roberts MA, Wadhams GH, Hadfield KA, Tickner S, Armitage JP.** 2012. ParA-like protein uses nonspecific chromosomal DNA binding to partition protein complexes. Proc. Natl. Acad. Sci. U. S. A. **109:**6698–6703. http://dx.doi.org/10.1073/pnas.1114000109.
8. **Guynet C, de la Cruz F.** 2011. Plasmid segregation without partition. Mob. Genet. Elements **1:**236–241. http://dx.doi.org/10.4161/mge.1.3.18229.
9. **Berry C, O'Neil S, Ben-Dov E, Jones AF, Murphy L, Quail MA, Holden MT, Harris D, Zaritsky A, Parkhill J.** 2002. Complete sequence and organization of pBtoxis, the toxin-coding plasmid of *Bacillus thuringiensis* subsp. *israelensis*. Appl. Environ. Microbiol. **68:**5082–5095. http://dx.doi.org/10.1128/AEM.68.10.5082-5095.2002.
10. **Tang M, Bideshi DK, Park HW, Federici BA.** 2006. Minireplicon from pBtoxis of *Bacillus thuringiensis* subsp. *israelensis*. Appl. Environ. Microbiol. **72:**6948–6954. http://dx.doi.org/10.1128/AEM.00976-06.
11. **Tinsley E, Khan SA.** 2006. A novel FtsZ-like protein is involved in replication of the anthrax toxin-encoding pXO1 plasmid in *Bacillus anthracis*. J. Bacteriol. **188:**2829–2835. http://dx.doi.org/10.1128/JB.188.8.2829-2835.2006.
12. **Larsen RA, Cusumano C, Fujioka A, Lim-Fong G, Patterson P, Pogliano J.** 2007. Treadmilling of a prokaryotic tubulin-like protein, TubZ, required for plasmid stability in *Bacillus thuringiensis*. Genes Dev. **21:**1340–1352. http://dx.doi.org/10.1101/gad.1546107.
13. **Ni L, Xu W, Kumaraswami M, Schumacher MA.** 2010. Plasmid protein TubR uses a distinct mode of HTH-DNA binding and recruits the prokaryotic tubulin homolog TubZ to effect DNA partition. Proc. Natl. Acad. Sci. U. S. A. **107:**11763–11768. http://dx.doi.org/10.1073/pnas.1003817107.
14. **Aylett CH, Lowe J.** 2012. Superstructure of the centromeric complex of TubZRC plasmid partitioning systems. Proc. Natl. Acad. Sci. U. S. A. **109:**16522–16527. http://dx.doi.org/10.1073/pnas.1210899109.
15. **Oliva MA, Martin-Galiano AJ, Sakaguchi Y, Andreu JM.** 2012. Tubulin homolog TubZ in a phage-encoded partition system. Proc. Natl. Acad. Sci. U. S. A. **109:**7711–7716. http://dx.doi.org/10.1073/pnas.1121546109.
16. **Park YN, Masison D, Eisenberg E, Greene LE.** 2011. Application of the FLP/FRT system for conditional gene deletion in yeast Saccharomyces cerevisiae. Yeast **28:**673–681. http://dx.doi.org/10.1002/yea.1895.
17. **Sambrook J, Russell DW.** 2001. Molecular cloning: a laboratory manual, 3rd ed. Cold Spring Harbor Laboratory Press, Cold Spring Harbor, NY.
18. **Thorne CB.** 1993. *Bacillus anthracis*, p 113–124. *In* Sonenshein AB, Hoch JA, Losick R (ed), *Bacillus subtilis* and other gram-positive bacteria: biochemistry, physiology, and molecular genetics. American Society for Microbiology, Washington, DC.
19. **Pomerantsev AP, Sitaraman R, Galloway CR, Kivovich V, Leppla SH.** 2006. Genome engineering in *Bacillus anthracis* using Cre recombinase. Infect. Immun. **74:**682–693. http://dx.doi.org/10.1128/IAI.74.1.682-693.2006.
20. **Pritzlaff CA, Chang JC, Kuo SP, Tamura GS, Rubens CE, Nizet V.** 2001. Genetic basis for the beta-haemolytic/cytolytic activity of group B Streptococcus. Mol. Microbiol. **39:**236–247. http://dx.doi.org/10.1046/j.1365-2958.2001.02211.x.
21. **Pomerantsev AP, Kalnin KV, Osorio M, Leppla SH.** 2003. Phosphatidylcholine-specific phospholipase C and sphingomyelinase activities in bacteria of the *Bacillus cereus* group. Infect. Immun. **71:**6591–6606. http://dx.doi.org/10.1128/IAI.71.11.6591-6606.2003.
22. **Ravel J, Jiang L, Stanley ST, Wilson MR, Decker RS, Read TD, Worsham P, Keim PS, Salzberg SL, Fraser-Liggett CM, Rasko DA.** 2009. The complete genome sequence of *Bacillus anthracis* Ames "Ancestor." J. Bacteriol. **191:**445–446. http://dx.doi.org/10.1128/JB.01347-08.
23. **Straub T, Baird C, Bartholomew RA, Colburn H, Seiner D, Victry K, Zhang L, Bruckner-Lea CJ.** 2013. Estimated copy number of *Bacillus anthracis* plasmids pXO1 and pXO2 using digital PCR. J. Microbiol. Methods **92:**9–10. http://dx.doi.org/10.1016/j.mimet.2012.10.013.
24. **Goios A, Meirinhos J, Rocha R, Lopes R, Amorim A, Pereira L.** 2006. RepeatAround: a software tool for finding and visualizing repeats in circular genomes and its application to a human mtDNA database. Mitochondrion **6:**218–224. http://dx.doi.org/10.1016/j.mito.2006.06.001.
25. **Okinaka RT, Cloud K, Hampton O, Hoffmaster AR, Hill KK, Keim P, Koehler TM, Lamke G, Kumano S, Mahillon J, Manter D, Martinez Y, Ricke D, Svensson R, Jackson PJ.** 1999. Sequence and organization of pXO1, the large *Bacillus anthracis* plasmid harboring the anthrax toxin genes. J. Bacteriol. **181:**6509–6515.
26. **Van der Auwera G, Mahillon J.** 2005. TnXO1, a germination-associated class II transposon from *Bacillus anthracis*. Plasmid **53:**251–257. http://dx.doi.org/10.1016/j.plasmid.2004.08.004.
27. **Livny J, Yamaichi Y, Waldor MK.** 2007. Distribution of centromere-like parS sites in bacteria: insights from comparative genomics. J. Bacteriol. **189:**8693–8703. http://dx.doi.org/10.1128/JB.01239-07.
28. **Kulinska A, Cao Y, Macioszek M, Hayes F, Jagura-Burdzy G.** 2011. The centromere site of the segregation cassette of broad-host-range plasmid RA3 is located at the border of the maintenance and conjugative transfer modules. Appl. Environ. Microbiol. **77:**2414–2427. http://dx.doi.org/10.1128/AEM.02338-10.
29. **Passalacqua KD, Varadarajan A, Ondov BD, Okou DT, Zwick ME, Bergman NH.** 2009. The structure and complexity of a bacterial transcriptome. J. Bacteriol. **191:**3203–3211. http://dx.doi.org/10.1128/JB.00122-09.
30. **Cong Q, Grishin NV.** 2012. MESSA: Meta-Server for protein Sequence Analysis. BMC Biol. **10:**82. http://dx.doi.org/10.1186/1741-7007-10-82.
31. **Lutkenhaus J.** 2012. The ParA/MinD family puts things in their place. Trends Microbiol. **20:**411–418. http://dx.doi.org/10.1016/j.tim.2012.05.002.

32. **Bramkamp M, Emmins R, Weston L, Donovan C, Daniel RA, Errington J.** 2008. A novel component of the division-site selection system of *Bacillus subtilis* and a new mode of action for the division inhibitor MinCD. Mol. Microbiol. **70:**1556–1569. http://dx.doi.org/10.1111/j.1365-2958.2008.06501.x.
33. **Patrick JE, Kearns DB.** 2008. MinJ (YvjD) is a topological determinant of cell division in *Bacillus subtilis*. Mol. Microbiol. **70:**1166–1179. http://dx.doi.org/10.1111/j.1365-2958.2008.06469.x.
34. **Eswaramoorthy P, Erb ML, Gregory JA, Silverman J, Pogliano K, Pogliano J, Ramamurthi KS.** 2011. Cellular architecture mediates DivIVA ultrastructure and regulates Min activity in *Bacillus subtilis*. mBio **2**(6):e00257–11. http://dx.doi.org/10.1128/mBio.00257-11.
35. **Gamba P, Veening JW, Saunders NJ, Hamoen LW, Daniel RA.** 2009. Two-step assembly dynamics of the *Bacillus subtilis* divisome. J. Bacteriol. **191:**4186–4194. http://dx.doi.org/10.1128/JB.01758-08.
36. **Vecchiarelli AG, Mizuuchi K, Funnell BE.** 2012. Surfing biological surfaces: exploiting the nucleoid for partition and transport in bacteria. Mol. Microbiol. **86:**513–523. http://dx.doi.org/10.1111/mmi.12017.